

Suppress carrier recombination by introducing defects: The case of Si solar cell

Yuan Yue Liu,^{1,a)} Paul Stradins,^{1,a)} Huixiong Deng,² Junwei Luo,² and Su-Huai Wei^{1,a),b)}

¹National Renewable Energy Laboratory, Golden, Colorado 80401, USA

²Institute of Semiconductors, Chinese Academy of Sciences, Beijing 100083, China

(Received 11 October 2015; accepted 24 December 2015; published online 11 January 2016)

Deep level defects are usually harmful to solar cells. Here we show that incorporation of selected deep level defects in the carrier-collecting region, however, can be utilized to improve the efficiency of optoelectronic devices. The designed defects can help the transport of the majority carriers by creating defect levels that are resonant with the band edge state, and/or reduce the concentration of minority carriers through Coulomb repulsion, thus suppressing the recombination at the carrier-collecting region. The selection process is demonstrated by using Si solar cell as an example. Our work enriches the understanding and utilization of the semiconductor defects.

© 2016 AIP Publishing LLC. [<http://dx.doi.org/10.1063/1.4939628>]

Defects play important roles in the performance of semiconductor devices. Although shallow level defects are often used to introduce charge carriers into semiconductors by doping, deep level defects are frequently found to be harmful in optoelectronic devices, such as solar cells, mainly because they can recombine charge carriers, decreasing the quantum efficiency of the device. Hence, significant efforts have been spent to minimize the amount of unwanted deep level defects. Here we show that, in contrast to conventional wisdom, adding selected deep level defects into the carrier-collecting region of a solar cell can actually improve the efficiency. The key is to find the proper defects, which can facilitate the transport of the majority carriers, and/or reduce the concentration of minority carriers at the carrier-collecting region. We demonstrate this idea by using the most common photovoltaic device—silicon solar cell—as an example.

Fig. 1 depicts a high efficiency cell structure.^{1,2} Electrons and holes photogenerated in Si are separated by the electric fields in p-n junction, and then ultimately collected by the metal contacts on both sides of the cell. As the quality of the solar wafer bulk improves up to ~10 ms bulk lifetime in record industrial-grade Si cells,³ the efficiency loss by the non-radiative recombination of electrons and holes at the surfaces and contacts becomes one of the bottlenecks. Due to the presence of a large density of gap states, metal/Si contacts are especially detrimental.⁴ Therefore, in a typical Si cell, most of the front area (>95%) is passivated by dielectric layers, such as SiO₂ or Al₂O₃, while only ~5% area constitutes metal/Si contact, which is kept to collect carriers. For high efficiencies, the back surface is typically also patterned by dielectric layer. A complete passivation of the Si back surface without metal patterning is realized in the HIT[®] cell,⁵ and more recently, in a tunneling passivated contact cell^{1,2} (Fig. 1), which results in record⁶ or close to record cell efficiency.⁷ In these cases, the carrier collection relies on

transport through the passivation layer of either intrinsic amorphous Si:H or SiO₂. For the case of amorphous Si:H, the transport occurs by thermionic transport over the respective band offsets,⁸ while for SiO₂, the transport is dominated by tunneling. Unfortunately, the passivation layer is not very conductive, which hinders the carrier collection and lowers the cell's fill-factor.⁵ Ideally, one would like to make the passivation layer conductive for majority carriers. In this work, by using the example of the high-efficiency Si solar cell shown in Fig. 1, we demonstrate (i) how one can engineer defect states in the dielectric layer adjacent to Si to enable efficient carrier transport through it while still retaining very high degree of passivation; this refers to the SiO₂ layer at the back of solar cell. We also show that (ii) for a surface dielectric layer that does not need to transport carriers yet has limited passivation quality due to the partial coverage of Si surface, the passivation quality can be improved by increasing the right built-in charge in the dielectric layer that repels

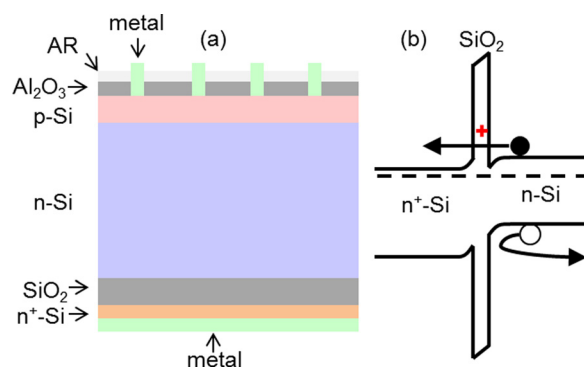


FIG. 1. Left: a high-efficiency Si solar cell structure, as described in Ref. 1. Front: B-diffused region with Al₂O₃ passivation and SiN_x anti-reflection (AR) layers, with metal grid directly contacting ~2% of the Si surface. Bottom: Full area tunneling contact with passivating SiO₂ interlayer and heavily P-doped poly-Si that both separate metal from the wafer. The top surface is usually textured (not shown) to maximize light absorption. Right: band alignment under illumination at the back surface. Filled circle denotes electron, and hollow circle represents hole. Defects in the SiO₂ layer are shown by + symbols, indicating they are positively charged. These defects can repel the holes, and help tunneling of the electrons.

^{a)}Authors to whom correspondence should be addressed. Electronic addresses: yuanyue.liu.microman@gmail.com; pauls.stradins@nrel.gov; and suhuaiwei@csrc.ac.cn

^{b)}Present Address: Beijing Computational Science Research Center, Beijing 100094, China

minority carriers (“field effect passivation”); this refers to the Al_2O_3 layer at the front of solar cell. In both cases, the defects can suppress the carrier recombination.

The transport through the passivation layer (case (i)) encounters a large barrier which is defined by the band offset between Si and the passivation material. If a defect in the passivation layer creates an energy level close to the Si band edge, then the barrier is reduced to the energy difference between the defect level and the Si band edge. In other words, carriers can “leak” through the passivation layer through these defects, therefore reducing the contact resistance. In addition, the defects should avoid creating electronic levels inside the Si band gap; otherwise they would cause recombination. Taking these two considerations into account, one concludes that, to assist the electron transport, ideally the defect level should be slightly above the conduction band minimum (CBM) of the absorber. Similarly, to help the hole transport, the defect level should be slightly below the valence band maximum (VBM). In case (ii), the passivation can be improved by reducing the concentration of minority carriers; this can be achieved by Coulomb repulsion between the minority carriers and the defects, which should have the same charge polarity. A high charge state of the defect is preferred as it gives rise to a stronger repulsion. Fig. 1(b) shows schematically an example of these “recombination-suppressing” defects, which can help the transport of electrons and repel holes simultaneously. In addition to these considerations, the effectiveness of defects can be affected by other parameters. For example, increasing the defects density in a reasonable range (without degrading the host material) can enhance their effects. Also, a large cross section for carrier capture could facilitate the carrier transport, and hence a more delocalized wave function for defect would be beneficial. These parameters suggest that it is possible to further tune the effectiveness of designated defects.

To identify promising defects, we perform first-principle calculations by using density functional theory (DFT) with projector augmented wave (PAW) pseudopotentials⁹ as implemented in VASP.¹⁰ A $3 \times 3 \times 3$ supercell of α -quartz (or α - Al_2O_3) is used to model the defects. The structures are fully relaxed by using Perdew–Burke–Ernzerhof (PBE) exchange–correlation functional¹¹ until the final force on each atom is <0.01 eV/Å. HSE functional¹² is then used to calculate the formation energy of the charged defect (referred to its neutral state)¹³

$$E_f(q) = E(q) - E(0) + \varepsilon_F,$$

where $E(q)$ is the total energy of the supercell containing a defect in charge state q , and ε_F is the Fermi level. The most stable charge state at given ε_F can then be identified by plotting $E_f(q)$ vs. ε_F for various q , and the cross points in the plot gives the charge transition level. In order to examine whether the defects could help the transport or not, we align the charge transition levels with respect to the Si band edge, by using the experimental band offset between Si and SiO_2 (or Al_2O_3).¹⁴

Figure 2 shows the calculated defect levels in SiO_2 . At the back of the cell, the contacting Si is n-type (Fig. 1(a)), and the Fermi level of the system lies close to Si CBM. As

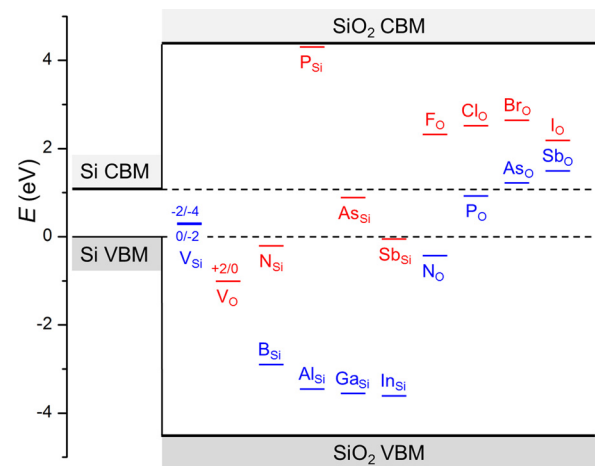


FIG. 2. Defect levels in SiO_2 , aligned with the band edges of Si. Unless specified, red bars show the transition levels of $+1/0$ and blue bars show the transition levels of $0/-1$.

mentioned before, the selected defects should assist the electron transport without causing additional efficiency loss. Clearly, Si vacancy (V_{Si}) in SiO_2 is undesirable as it has levels within the Si band gap, which would induce recombination. In contrast, the O vacancy (V_{O}) creates levels outside the Si band gap. However, it helps the tunneling of holes instead of electrons, because it has a level located below the Si VBM, and thus is not a beneficial defect for the n-type contact. Substituting Si by group III elements (B, Al, Ga, and In) creates negatively charged defects that repel electrons, impeding the electron collection. Substituting Si by group V elements (N, P, As, and Sb) is also not a good choice, because their levels are either inside Si band gap, below the Si VBM, or far above the Si CBM. O substitution by N or P is also detrimental because it creates negatively charged defects; in particular, P_{O} level falls inside Si band gap. However, As_{O} and Sb_{O} remain neutral, and their levels are slightly above Si CBM, and are thus good candidates for facilitating electron transport. O substitution by group VII elements (F, Cl, Br, and I) is also appealing, as it creates levels close to the Si CBM, and can repel the holes due to its positive charge. The above considerations can be applied also to p-type (hole collecting) passivated contact with SiO_2 tunneling layer, which can be used in cell architectures other than Fig. 1—for example, inverted cell with p-n junction at the bottom and diffused n+/n-junction at the front, or an interdigitated back contact cell. For such p-type contact, V_{O} , N_{Si} , N_{O} , B_{Si} , Al_{Si} , Ga_{Si} , In_{Si} , and Sb_{Si} appear beneficial.

It is interesting to notice that Sb_{O} shows the highest level in group V elements, while I_{O} has the lowest level in group VII elements. In general, for anions in the same group, as the atomic number increases, the orbital energy increases, raising the defect level.¹⁵ On the other hand, the atomic size also becomes larger, which weakens the coupling between the defects and the host, therefore decreasing the energy of anti-bonding state and increasing of the energy of the bonding-state.¹⁵ O substitution by group V elements creates bonding states; thus, both the orbital energy and the size effects contribute to the increase of the defect level as the atomic number increases. Consequently, Sb_{O} has the highest level. In contrast, O substitution by group VII elements creates

anti-bonding states. Although I_O has a high orbital energy, it also has the largest size and therefore the weakest coupling, which overcomes its high orbital energy, resulting in the lowest level.

In reality, the selected defects (As_O , Sb_O , F_O , Cl_O , Br_O , and I_O) can be located not only in the SiO_2 bulk, but also at the interface between Si and SiO_2 . This might affect the passivation quality of Si surface. To examine this effect, we take the most stable Si– SiO_2 interface structure from Ref. 16, as shown in Fig. 3. Without defects, all the Si surface dangling bonds are fully saturated by O, and no intermediate states are found between the Si VBM and CBM, confirming the excellent passivation by SiO_2 . Surprisingly, even with the selected defects (As_O , Sb_O , F_O , Cl_O , Br_O , and I_O) at the interface, there are still no gap states. This is consistent with the calculations for defects in bulk SiO_2 (Fig. 2), which indicates that their levels are outside Si band gap. Interestingly, these substituting elements form only two bonds with Si, unlike their usual chemical coordination. This is because the defect accepts or donates one electron to the bulk Si, resulting in two unpaired electrons and therefore forming only two bonds. Consequently, the selected defects do not deteriorate the surface passivation of Si even if they are positioned at the interface.

In case (ii), the requirements for beneficial defects are different from those of case (i): the defects levels should lie outside the Si energy gap and repel minority carriers in the p-type emitter (electrons) from the Si/metal interface. To achieve the latter function, the selected defects in Al_2O_3 should carry negative charge as much as possible. This reduces the recombination via the Si/metal interface states. Since the contacting Si is p-type, Fermi level of the system lies close to the Si VBM. Fig. 4 shows the defect levels in Al_2O_3 . In order to make the defects negatively charged, the substitutional elements should have lower valence state than the substituted atoms, for example, replacing O by group V elements. However, this does not necessarily lead to negatively charged defects, as can be seen from the neutral P_O and As_O . We also consider the cation dopants which are compatible with the process of atomic layer deposition

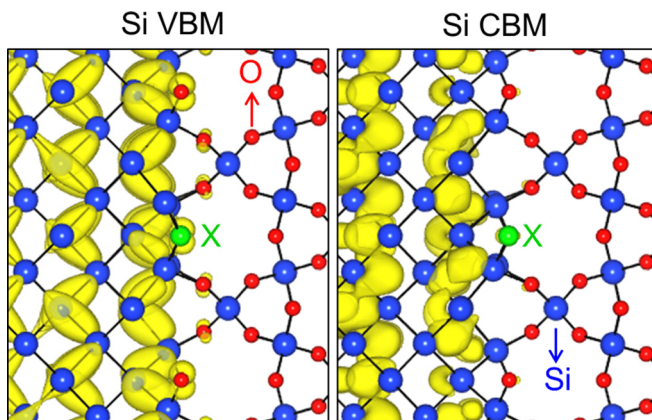


FIG. 3. Atomic structure of Si– SiO_2 interface (Si: blue; O: red; and substitutional atom: green) and the charge density distribution (yellow isosurface) of Si VBM and CBM. Our calculations show that there is no additional electronic state between Si VBM and CBM. For each panel, the materials on the left are Si and on the right are SiO_2 .

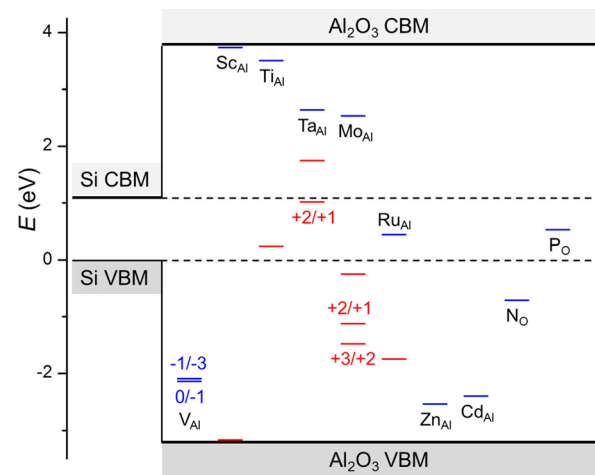


FIG. 4. Defect levels in Al_2O_3 , aligned with the band edges of Si. Unless specified, red bars show the transition levels of $+1/0$, and blue bars show the transition levels of $0/-1$.

(ALD) as the Al_2O_3 are grown by ALD.¹⁷ Most of these defects are not negatively charged (Sc_{Al} , Ti_{Al} , Ta_{Al} , Mo_{Al} , and Ru_{Al}). This is because they have either the same or higher valence state in oxides compared with Al ($+3$). In contrast, Zn and Cd have a valence of $+2$, therefore resulting in a -1 charge state for Zn_{Al} and Cd_{Al} . Al vacancy (V_{Al}) turns out to have the most negative charge of -3 . Therefore, growing Al_2O_3 layer under Al-poor condition could help improve the cell efficiency. We note that experimentally the Al_2O_3 layer provides very good passivation to p-type Si due to the built-in negative charge.¹⁸ The origin of the latter appears to be related with non-stoichiometric interface located at the interface between the stoichiometric Al_2O_3 layer and a very thin SiO_x layer that forms unintentionally between the Al_2O_3 and wafer.¹⁹ The non-stoichiometric interface is found to be oxygen rich,¹⁹ implying possible formation of V_{Al} . This is consistent with our calculations showing that V_{Al} has a strong negative charge.

It should be noted that the defects may change the optical properties of the host material, in which cases the photons excite transition between defect levels and CBM/VBM of SiO_2/Al_2O_3 . However, this is not a concern for back contact SiO_2 , where negligible sunlight can reach. For front contact Al_2O_3 , although the suggested V_{Al} defect has electrons which can be excited to the CBM of Al_2O_3 , Fig. 3 shows that this transition needs photon energy >5 eV. Therefore, it would not cause significant parasitic absorption.

Experimentally, the designated defects could be introduced by plasma enhanced chemical vapor deposition (which has been used to introduce F into SiO_2),²⁰ ion implantation,²¹ thermal or plasma nitridation, oxidation of a impurity-enriched layer of Si wafer, or ALD with various precursors containing the desired elements.¹⁷

The idea of adding defects to assist the transport of majority carriers and/or repel the minority carriers opens possibilities to combine good surface passivation with enhanced carrier transport. Tunneling layers thus could be made thicker, less prone to process uncertainties and spatial inhomogeneities. Besides solar cells, they could also be applied to other devices. For example, Hu *et al.*²² have recently

shown that by coating a “defective” TiO₂ layer of 4 to 143 nm, the Si, GaAs, and GaP photoanodes are chemically stabilized with a high efficiency for water oxidation. This is possibly due to the excellent passivation of the semiconductor surfaces by TiO₂, as well as the efficient hole transport assisted by the defects.

In summary, by using Si solar cell as an example, we demonstrate that the incorporation of selected defects can be utilized to improve the efficiency of photovoltaic device. Specifically, we have identified defects that can facilitate the transport of majority carriers, and/or repel the minority carriers, thus suppressing the recombination at the carrier-collecting region. Our work, therefore, enriches the understanding and utilization of the semiconductor defects.

This work is supported by the U.S. DOE (DE-EE0006336, FPACE-II). This work used the NREL Peregrine Supercomputer, as well as the National Energy Research Scientific Computing Center (NERSC), which is supported by the Office of Science of the U.S. Department of Energy under Contract No. DE-AC02-05CH11231. The authors gratefully acknowledge discussions with collaborators Arrelaine Dameron, Ajeet Rohatgi, Martin Hermle, and Jan Benick. This research was funded by the U.S. Department of Energy under Contract No. DE-AC36-08GO28308.

¹F. Feldmann, M. Bivour, C. Reichel, M. Hermle, and S. W. Glunz, *Sol. Energy Mater. Sol. Cells* **120**, 270 (2014).

²B. Nemeth, D. L. Young, Y. Hao-Chih, V. LaSalvia, A. G. Norman, M. Page, B. G. Lee, and P. Stradins, in 2014 IEEE 40th Photovoltaic Specialist Conference (PVSC), 2014.

³D. D. Smith, P. Cousins, S. Westerberg, R. De Jesus-Tabajonda, G. Aniero, and S. Yu-Chen, *IEEE J. Photovoltaics* **4**(6), 1465 (2014).

- ⁴J. Benick, B. Hoex, M. C. M. van de Sanden, W. M. M. Kessels, O. Schultz, and S. W. Glunz, *Appl. Phys. Lett.* **92**(25), 253504 (2008).
- ⁵S. De Wolf, A. Descoedres, Z. C. Holman, and C. Ballif, *Green* **2**(1), 7 (2012).
- ⁶K. Masuko, M. Shigematsu, T. Hashiguchi, D. Fujishima, M. Kai, N. Yoshimura, T. Yamaguchi, Y. Ichihashi, T. Mishima, N. Matsubara, T. Yamanishi, T. Takahama, M. Taguchi, E. Maruyama, and S. Okamoto, *IEEE J. Photovoltaics* **4**(6), 1433 (2014).
- ⁷F. Feldmann, M. Bivour, C. Reichel, H. Steinkemper, M. Hermle, and S. W. Glunz, *Sol. Energy Mater. Sol. Cells* **131**, 46 (2014).
- ⁸J. P. Seif, A. Descoedres, M. Filipič, F. Smole, M. Topič, Z. C. Holman, S. De Wolf, and C. Ballif, *J. Appl. Phys.* **115**(2), 024502 (2014).
- ⁹G. Kresse and D. Joubert, *Phys. Rev. B* **59**(3), 1758 (1999); P. E. Blöchl, *ibid.* **50**(24), 17953 (1994).
- ¹⁰G. Kresse and J. Hafner, *Phys. Rev. B* **47**(1), 558(R) (1993); G. Kresse and J. Furthmüller, *ibid.* **54**(16), 11169 (1996).
- ¹¹J. P. Perdew, K. Burke, and M. Ernzerhof, *Phys. Rev. Lett.* **77**(18), 3865 (1996).
- ¹²J. Paier, M. Marsman, K. Hummer, G. Kresse, I. C. Gerber, and J. G. Ángyán, *J. Chem. Phys.* **124**(15), 154709 (2006).
- ¹³S.-H. Wei, *Comput. Mater. Sci.* **30**(3–4), 337 (2004).
- ¹⁴E. Bersch, S. Rangan, R. A. Bartynski, E. Garfunkel, and E. Vescovo, *Phys. Rev. B* **78**(8), 085114 (2008).
- ¹⁵S.-H. Wei and S. B. Zhang, *Phys. Rev. B* **66**(15), 155211 (2002).
- ¹⁶R. Buczko, S. J. Pennycook, and S. T. Pantelides, *Phys. Rev. Lett.* **84**(5), 943 (2000).
- ¹⁷V. Miikkulainen, M. Leskelä, M. Ritala, and R. L. Puurunen, *J. Appl. Phys.* **113**(2), 021301 (2013).
- ¹⁸G. Dingemans and W. M. M. Kessels, *J. Vac. Sci. Technol. A* **30**(4), 040802 (2012).
- ¹⁹V. Naumann, M. Otto, R. B. Wehrspohn, M. Werner, and C. Hagendorf, *Energy Procedia* **27**, 312 (2012).
- ²⁰S. W. Lim, Y. Shimogaki, Y. Nakano, K. Tada, and H. Komiyama, *Appl. Phys. Lett.* **68**(6), 832 (1996); D. R. Denison, J. C. Barbour, and J. H. Burkhart, *J. Vac. Sci. Technol. A* **14**(3), 1124 (1996).
- ²¹C. Reichel, F. Feldmann, R. Müller, R. C. Reedy, B. G. Lee, D. L. Young, P. Stradins, M. Hermle, and S. W. Glunz, *J. Appl. Phys.* **118**(20), 205701 (2015); A. H. van Ommen, *ibid.* **61**(3), 993 (1987).
- ²²S. Hu, M. R. Shaner, J. A. Beardslee, M. Lichterman, B. S. Brunschwig, and N. S. Lewis, *Science* **344**(6187), 1005 (2014).